EFFECT OF CORROSION ON END REGION BEHAVIOR OF PRETENSIONED, PRESTRESSED BRIDGE GIRDERS

Darion T. Mayhorn, Bureau of Reclamation, Denver, CO
Cameron D. Murray, University of Oklahoma, Norman, OK
Royce W. Floyd, Ph.D., P.E., University of Oklahoma, Norman, OK
Gary S. Prinz, Ph.D., P.E., University of Arkansas, Fayetteville, AR

ABSTRACT

Corrosion damage in the end regions of pretensioned, prestressed concrete bridge girders is a common problem for bridges with deck joints over the girder ends, but limited information is available on the effect of varying levels of strand corrosion on end region behavior. Nine half-scale prestressed girders were constructed to replicate AASHTO Type II girders representative of a large number of aging bridges, and were tested to examine the effects of end region deterioration on strand anchorage and shear capacity. Two different girder designs were utilized, corresponding to the different prestressing strand configurations used for two full-scale girders tested in shear as part of a separate, larger project. One end region of each scaled girder was exposed to an accelerated corrosion process, and four different exposures were used to represent varying environmental conditions. The end regions of six of the girders were then shear tested after damage by corrosion and two are still under exposure. In general, the levels of corrosion damage tested did not appreciably reduce the capacity of the girders, but did affect the failure mechanism.

Keywords: End-region, Corrosion, Shear, Anchorage, Prestressed, Concrete

INTRODUCTION

The end regions of prestressed concrete girders play an important role in the overall function of the design. In the end regions of pretensioned girders, the load is transferred to the beam through bond between the prestressing strands and the concrete. This force distribution, known as prestress transfer, requires higher concentrations of mild steel reinforcement in the end region to resist "splitting" of pretensioned members. Additionally, greater shear demand at the ends and reduced prestress force within the transfer length creates a need for more transverse reinforcement. The girder end region's high percentage of steel combined with being located near the joints of the bridge deck, which provide a path for water and chlorides from deicing salts to reach the girder ends, makes the end region more susceptible to corrosion than the remainder of the girder. Continued exposure over the life of the bridge can lead to corrosion of this reinforcing steel in the end regions. Any damage due to corrosion in this region could have a lasting impact on the girder's overall strength, especially the shear capacity.

Bridges designed 30-50 years ago typically used the American Association of State Highway and Transportation Officials (AASHTO) Standard Specifications to design prestressed girders. In the past, AASHTO recommended a "quarter-point rule" for shear design, which often produced a potentially less conservative design than the current specifications. The "quarter-point rule" considered the critical section for shear to be at one quarter (1/4) of the span length, and allowed all sections between the end and the quarter-point to be designed using the applied shear at the quarter-point. The current AASHTO Load and Resistance Factor Design (LRFD) Specifications[1] specify that the critical section for shear be located at a distance equal to the effective shear depth, d_v, from the supports. This change in design codes has a potentially large impact on shear demand, thus the adequacy of the end regions of older bridges relative to shear may be influenced by the previous design code. These older bridges may be more of a concern when they also exhibit deterioration of the beam ends due to corrosion. It is therefore important to have an adequate understanding of the behavior of members exhibiting corrosion and the prevalence of such corroded members in in-service bridges.

Chlorides are particularly damaging for concrete and appurtenant embedded materials as they reduce the effectiveness of the concrete's alkalinity which normally protects the steel from corrosion. Chlorides can be introduced to concrete through use of chloride as an accelerant, use of water containing chloride, contaminated aggregates, sea salt spray, and use of chemicals and de-icing salts.[2] A survey of bridges used in salt de-icing environments illustrated that the majority of chloride-induced corrosion over time was due to "chloride-laden water" from the bridge deck that trickled through expansion joints, cracks in the deck concrete overlay, and inadequately designed concrete cover.[2] While researching chloride ion distribution in 20-year-old prestressed concrete girders in Minnesota, Coggins and French[3] found that the only evidence of strand corrosion was observed at the ends of the beams. Smith and Virmani[4] noted the ability to minimize the number of deck joints as a means to reduce the availability of seepage paths for chlorides to reach a bridge's superstructure and

substructure. Vu et al.[5] found that concrete cover and water-cement ratio (*w*/*c*) were good predictors for performance of chloride contaminated concrete related to cracking.

Corrosion of steel in concrete can cause many concerns including cracking, delamination, spalling of the concrete and loss of tensile strength of the steel embedded in the concrete. In order to prevent corrosion, reinforcing steel in most structures is now coated with materials (typically epoxy) to prevent, or at least delay, the corrosion process. For bridges constructed in the mid-1900s, which are now reaching the end of their design lives, epoxy was not applied to reinforcing steel, and almost certainly never applied to prestressing strands. One major consequence of deterioration in concrete caused by prestressing steel corrosion is the potential for reduction of the live load capacity. This capacity is impacted by both the reduction of the steel cross-section and loss of bonding between the concrete and steel. In their study on the bond of reinforcing bars subjected to accelerated corrosion, Abosrra et al.[6] found that the first day of corrosion acceleration caused a slight increase in steel/concrete bond strength. However, after 7 and 15 days of corrosion acceleration there was significantly reduced steel/concrete bond strength. In a study focused on deterioration of prestressed concrete bridge beams, Bruce et al.[7] concluded that corrosion in prestressing strands reduces the structural performance of a beam faster than corrosion exhibited in conventional reinforced beams because a larger proportion of the steel cross-section is lost. Szilard[8] emphasized that prestressing steel is also subjected to significantly higher stresses with smaller diameters in relation to conventional reinforcement.

Several recent studies have investigated the capacity of decommissioned bridge beams with corrosion damage. Rogers et al.[9] performed destructive tests on 19, 40-year-old pretensioned concrete beams that had corroded pretensioned reinforcement. Their results indicated that "the most severely corroded beam sustained 69% of the load of an equivalent good-condition beam."[9] El-Batanouny et al.[10] found that pitting corrosion in prestressed strands caused a reduction in residual capacity in only 140 days. They found that the most corroded member had a tested capacity of 86.7% when compared to the original control specimen.[10] Pape and Melchers[11] found that as the degree of corrosion loss in the prestressing strands increased, the maximum capacity of the girder decreased linearly. In determining the performance of three 45-year-old corroded prestressed concrete beams, the researchers concluded that using current design theory, estimated material properties, and neglecting cracking and corrosion damage ultimately overestimates the actual capacity of the beams. In one beam, they found that a 64% loss in prestressing cross-sectional area due to corrosion at the failure location contributed to a 49% reduction in original, theoretical design capacity.[11]

The research described in this paper is intended to expand on the current body of knowledge surrounding corrosion of prestressed concrete girders due to extreme environments, with particular focus on how end region deterioration ultimately affects the girder's shear capacity.

EXPERIMENTAL DESIGN

The laboratory testing consisted of the following process: construction of the prestressed concrete girders, end region deterioration of those girders through exposure to a highly corrosive environment, and shear testing of the girders. Nine prestressed concrete girder specimens were used for testing in this project. Six were shear tested, two are currently still being subjected to the corrosive environment, and one was saved to test potential retrofit methods.

PRESTRESSED CONCRETE GIRDER SPECIMENS

The prestressed concrete girder specimens were designed to be roughly half-scale AASHTO Type II girders with similar concrete compressive strength and in-service stress state as two full-scale decommissioned girders taken from the I-244 bridge over the Arkansas River in Tulsa, Oklahoma, and tested as part of a complementary project.[12] These full-scale girders are referred to as Beam “A” and Beam “C” in this paper based on the original design drawings of the decommissioned bridge. Reinforcing steel for the scale specimens was also designed to follow the reinforcement configuration of the original Beam “A” and Beam “C”. Since shear capacity of prestressed concrete beams is affected by the effective prestress, the scale girder designs were developed by adjusting the prestress configuration for the half-scale girder specimens to obtain service level stress states, based on effects of prestress and dead load, equivalent to that of the full-scale girders within an acceptable range. The girders were designed through multiple iterations using a design spreadsheet based on the ACI[13] and AASHTO[1] methods and developed as part of the complementary project.[12] The design spreadsheet considered the concrete stress at release and in service.

The final design intended to match Beam “A” (termed Girder A) included two ½ in. special strands spaced 2 in. apart and located 4 in. from the bottom of the section with a 186 ksi prestress. The final design intended to match Beam “C” (termed Girder C) included two 0.6 in. strands spaced 2 in. apart and located 4 in. from the bottom of the section with a 202.5 ksi prestress. Both of these designs produced service level compression stresses at the bottom fiber within 5 percent of the in-service stresses estimated for Beam “A” and Beam “C”, while the stresses at the tops of the beams differed by approximately 50% and 70% for the A and C designs respectively. However, a mistake made during construction of the formwork for the girders caused the depth of the girder to be 4.5 in. greater than anticipated, which affected the stresses in the actual specimens. A clear limitation of this study is that the prestressing strands were not scaled equally with the specimens. Small-diameter prestressing strands were not available for specimen construction creating an incompatibility in the strand transfer length relative to the specimen depth and loading location, compared to the full-size specimen. These factors would create an inherent difference in bond stress behavior compared to the full-size specimens.

Both designs included consideration of pretensioned anchorage zone reinforcement requirements and consistent concrete-to-steel shear strength contribution ratios between the full-scale and half-scale specimens. For the full-scale Beam “A,” the total nominal shear strength was provided by approximately 30% contribution from the concrete and 70% from

the transverse reinforcing steel. Similarly, for the full-scale Beam "C" the contributions were approximately 29% from the concrete and 71% from the steel. The concrete-to-steel strength ratios, presented in Table 1, were determined using the design spreadsheet along with the transverse steel spacing and bar sizes at a distance equal to ¼ of the span from the support and h/2 from the support. These locations were chosen to correspond to the older AASHTO requirements and the current ACI requirements. Final shear reinforcement consisted of single No. 3 Z bars spaced at 4 in. on center.

Table 1. Concrete-to-steel strength contribution ratios

Specimen Type	L/4 from the support		h/2 from the support	
	Concrete Contribution	Steel Contribution	Concrete Contribution	Steel Contribution
Beam "A" (full scale)	31%	69%	28%	72%
Girder A (half-scale)	26%	74%	26%	74%
Beam "C" (full scale)	29%	71%	29%	71%
Girder C (half-scale)	19%	81%	18%	82%

The concrete mix utilized to construct the beams was chosen to have a compressive strength comparable to the original concrete design used for the full-scale girders. The final mix design was based on a self-consolidating concrete used for other projects by the authors, had a water/cement (*w*/*c*) ratio of 0.37, no entrained air, and a theoretical unit weight of 150.9 lb/ft^3. Table 2 presents the final proportions used for the concrete mix design. No entrained air was included due to concern for consistency between mixes. The exclusion of entrained air would reduce the permeability of the concrete, providing a less representative case for chloride ingress than likely observed in the field. Concrete compressive strength tests were performed using 4 in. x 8 in. cylinders at intervals of 1 day, 7 days, and 28 days for quality control purposes and to ensure the required compressive strength for the girders was achieved.

Table 2. Concrete mix proportions used for casting girder specimens

Material	Quantity
Cement (lb/yd^3)	851
Sand (lb/yd^3)	1459
Rock (lb/yd^3)	1372
Water (lb/yd^3)	315
w/c	0.37
HRWR (oz/cwt)	5.0

The girders were cast using the prestressing bed at the Donald G. Fears Structural Engineering Lab over a period of five weeks. Ten, 18-ft long girders were cast: four using the Girder A design (only three of these were used due to poor consolidation for the first girder cast), and six using the Girder C design. Prestress force was released at roughly 24 hours, or when the concrete compressive strength reached 4 ksi. The girders were cured for at least 28 days inside Fears Lab and then taken outside in preparation for exposure to the corrosive environment. In order to replicate field conditions, the prestressing strands on the corrosion induced end were ground flush with the ends of the girders. Companion compressive strength

cylinders were stored alongside the completed girders throughout the curing and exposure process.

ACCELERATED CORROSION EXPOSURE

After the girders reached an age of 28 days, they were placed in a corrosive environment consisting of a chloride solution spray to induce end-region corrosion. The use of a chloride spray was intended to simulate the effect of a leaking expansion joint on the ends of the girders similar to that described by previous research[3,4] and observed by the authors in the field. No end diaphragms or other concrete cover was included on the ends of the beams, as would be present in the field, in order to speed up the corrosion process. Initially, a literature review was performed to understand chloride solutions successfully used for similar applications in previous research, as well as the optimum duration for wet/dry cycles of chloride saturated water.[6,14] Ultimately, a 5 percent by weight sodium chloride solution was used as the corrosive agent. A large plastic tub was used as a reservoir, with a submersible pump to circulate the chloride solution over one end of the beams. Perforated plastic tubes were bonded to the beams approximately 6 in. from the beam ends to correlate with the typical distance exposed to leaking joints observed by the authors for beams in the field. The perforations consisted of four 3/32 in.-diameter holes spaced to evenly spray the chloride solution over the beam ends. A valve was used to control the flow rate of the chloride solution through the perforated tubing. The final arrangement is shown in Figure 1. A cycle time of two hours on and two hours off was chosen based on the literature review, limitations of available timers, and to ensure drying between cycles.

Figure 1. Completed girders placed in corrosion accelerant setup (red arrows indicate the direction of flow from the perforated tubes)

One specimen from each girder design (A and C) was placed under accelerated corrosion for two months, four months, six months, and two years (still in process). After this corrosion

regimen, the girders were removed and prepared for shear testing. Figure 2 is an example of a corroded beam end after six months of the accelerated corrosion process. Rust staining is clearly visible on the surface of the beams at the location of the mild steel shear reinforcement and below the exposed strand ends. An autopsy of the corroded specimens to determine how far the corrosion extended into the beams was not conducted during this analysis.

Figure 2. Example of a corroded beam end after the accelerated corrosion process.

SHEAR TESTING OF CORRODED SPECIMENS

Following the accelerated corrosion period for the 2 month, 4 month and 6 month specimens, each end of each exposed specimen was tested in shear. A three point bending arrangement using a hydraulic actuator to apply load to the girder specimens was used and the untested end of the beam was cantilevered over the support to prevent damage during the first test of each specimen. The loading arrangement for shear was based on a shear span to depth (a/d) ratio of 2.0, intended to induce a bond-shear type failure. However, the chosen a/d ratio is at the border line of creating a discontinuity region for the entire section between the applied load and the nearest support, which could affect the applicability of typical capacity prediction equations. The support nearest the load point was located 4 in. from the end of the beam and the center-to-center distance between the supports was 9 ft, leaving 8 ft - 8 in. of overhang on the untested side. A single point load was applied through a 6 in. wide plate, centered 41 in. from the end of the beam. Sand was placed between the load plate and the beam to ensure uniform load distribution. The girders were loaded in 5000 lb increments before initial cracking and 2000 lb increments after initial cracking until failure.

Deflection at the load point was measured using wire potentiometers (wire pots) on each side of the beam. Strand end slip was measured using linear voltage differential transformers (LVDTs) attached to the prestressing strands on the non-corroded end and placed touching the strand ends on the corroded end. Manual deflection measurements were also taken after each load increment using a steel ruler. Visual mapping of cracking was conducted during the testing by marking cracks with a permanent marker and noting the load increments. Data were collected from all instruments during testing using a single data acquisition system. The data were used to compare the findings to the nominal strengths calculated using the ACI[13] and AASHTO LRFD[1] methods and to identify the failure mechanism. A strut and tie model was also considered for the beam end region to account for the loading configuration creating a discontinuity region at the end of the beam. The results of tests of the undamaged ends of the girders were compared to tests of the corroded girder ends to identify differences in performance. Figure 3 illustrates the shear test setup.

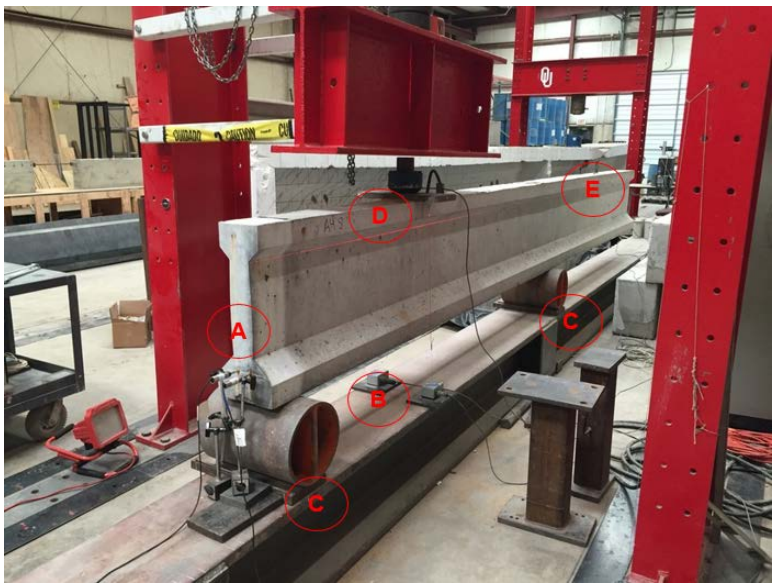

Figure 3. Typical shear test setup looking towards the north – (A) LVDT 1 & 2, (B) wire pots 1 (west) & 2 (east), (C) supports at 9 ft center-to-center, (D) single load point with load cell at 41 in. from end of beam, and (E) 8 ft - 8 in. overhang of the beam

RESULTS

COMPRESSIVE STRENGTH OF GIRDER CONCRETE

All of the measured concrete compressive strengths were larger than the targeted compressive strength of 4,000 psi at prestress release (1-day). However, there was a relatively large variation in the measured strengths, with the maximum value being more than 50% larger than the target. The compressive strength of Girder A4 was 4% less than the design compressive strength of 6,000 psi at 28-days. The remaining girders exceeded the design compressive strength, but with relatively large variation. The maximum value was 37% greater than the design compressive strength. The variation in compressive strength has

the potential to affect the prestress transfer and development lengths, as well as the girder's shear capacity. Larger compressive strengths could lead to shorter transfer and development lengths, and higher shear capacity.[16] These variations must be considered when interpreting the results.

SHEAR TESTS

For the discussion to follow, the location of the shear test is abbreviated as follows: first the girder specimen identification number (i.e., A4), then the end of the girder (i.e., north or south), and lastly if it is the "corroded end" then a "C" follows. The label for the end of the girder identifies the location in the prestressing bed. The label is also significant in that the accelerated corrosion process was not consistently applied on one directional end (i.e., not all of the girders were corroded on the north end of the girders). As an example, in describing the corroded south end of Girder A4, the abbreviation is A4SC. A summary of the results of all shear tests is given in Table 3. The failure types listed are based on the terminology recommended by Naji et al.[16]. The majority of failures were due to a combination of strand bond and shear cracking, typically with one caused by other.

Table 3. Failure mechanisms of girders during each shear test

Specimen	Test Age	Corroded End	Control End
Girder A4	2 months	Bond-shear failure; slip before flexural cracking	Bond-shear failure; flexural-shear cracking before slip
Girder C1	2 months	Bond-shear failure; slip before web-shear cracking	Bond-shear/flexure failure; flexural-shear cracking before slip; flange deterioration
Girder A3	4 months	Bond-shear failure; slip before flexural cracking	Bond-shear failure; maybe flexural failure first; flexural-shear cracking before slip
Girder C2	4 months	Bond-shear failure; slip before web-shear cracking	Bond-shear failure; cracking before slip
Girder A2	6 months	Web-shear failure; flexural cracking initially	Bond-shear failure; web-shear cracking before slip
Girder C3	6 months	Bond-shear/flexure failure; web-shear cracking before slip; concrete crushed at load point	Bond-shear failure; web-shear cracking before slip

The measured cracking load and failure load were determined via the notes taken during testing, along with the load-deflection data provided from the data acquisition system. Figure 4 illustrates the varying failure loads by girder design. Overall, the corroded ends of the

girder specimens with the Girder A design sustained larger failure loads than those corroded ends of the girders with the Girder C design. All failures were primarily due to combination of bond and shear cracking caused in part by the design of the test and exacerbated by the large diameter strands used compared to the cross-section size and their development length compared to the load location. The larger 0.6 in. strands used in the Girder C design likely contributed to earlier slip and reduced capacity compared to the specimens with 0.5 in. special strands.

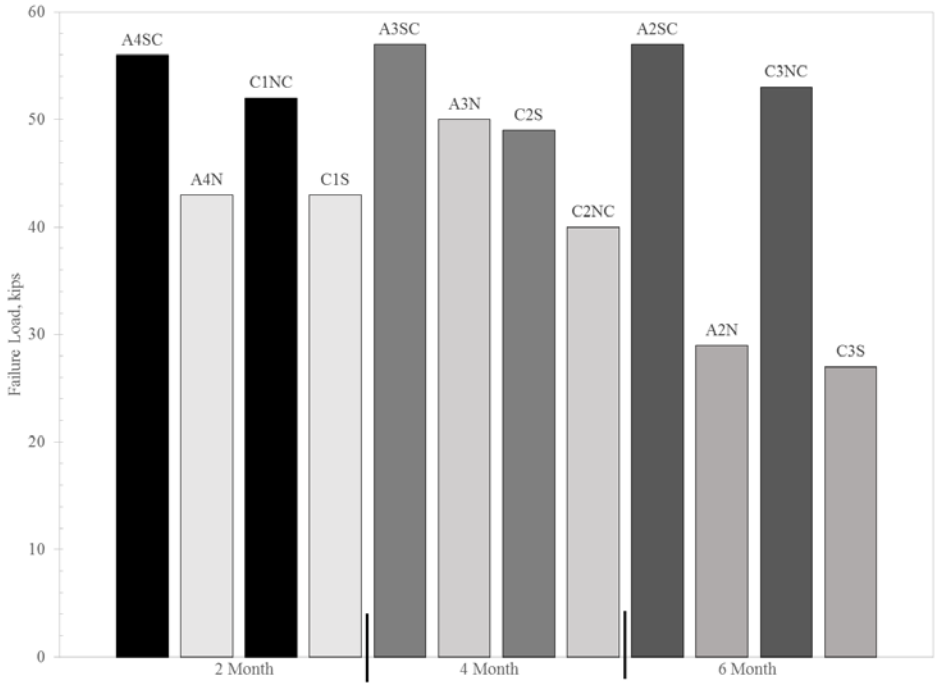

Figure 4. Comparison of failure loads for Girder A and Girder C designs

All of the corroded ends, except for girder specimen C2, had a larger measured shear than the control end. This behavior is similar to results reported by Abosrra et al. for minor corrosion.[6] With the exception of girder specimen C2, the corroded end of each girder was tested first. The order of testing could potentially have impacted the condition of the beam, thereby impacting the remaining end and resulting in less resistance available for the control ends. Shear capacity may have been larger at the corroded ends of the girders due to larger compressive strength from additional curing moisture provided by the accelerated corrosion process. A higher compressive strength could also result in better strand anchorage within the transfer length and greater resistance to strand pullout during testing. No additional curing water was provided for the rest of each specimen, so the control ends potentially had a lower compressive strength in the anchorage zone. No cores were taken to confirm this hypothesis before the beams were discarded, but cores are planned for the final two beams to be tested after two years of exposure. Strand slip was observed for all specimens, which caused the beams to fail sooner than they otherwise would have. For at least four of the corroded ends of the girder specimens, the prestressing strands slipped prior to initial observed cracking indicating a potential effect on the strand bond. However, the increased surface roughness caused by corrosion, without observed section loss, may have increased the overall

anchorage capacity for the specimens tested. All control ends exhibited cracking before strand slip was observed. At least one horizontal crack was observed near the level of the prestressing strands before testing for nearly all of the specimen ends. It is possible that the increase in roughness from corrosion provided an improvement in anchorage relative to these cracks compared to the control ends. The control ends of girder specimens A2 and C3, exposed for six months, had a significantly smaller measured shear than the other tested control ends. There is no clear evidence as to why this occurred, but may be related to horizontal cracks present before testing.

Table 4 shows the estimated flexural and shear capacity values for each girder specimen to the measured values for each shear test. For example, for specimen A4SC, the failure load (P_{max}) of 56 kips corresponds to a maximum applied moment (M_{max}) of 113 k-ft., and a maximum applied shear (V_{max}) of 36.5 kips. The estimated values for specimen A4SC are 126.2 kip-ft for the moment capacity (M_n) calculated using strain compatibility, 45.5 kips for the shear capacity (V_n) using the AASHTO LRFD 2007 method[17], 27.2 kips for the shear capacity (V_n) using the AASHTO LRFD 2012 method[1], 53.4 kips for the shear capacity (V_n) using the ACI detailed method[13], and a maximum load of 30.5 kips based on a strut and tie model of the end region. Figure 5 illustrates the design and measured shear values for each girder for comparison.

Table 4. Design and experimental capacity values for each shear test specimen

Test	P_{max} (kips)	M_{max} (kip-ft)	V_{max} (kips)	P_n S&T (kips)	M_n (kip-ft)	V_n LRFD 2007 (kips)	V_n LRFD 2012 (kips)	V_n ACI (kips)
A4SC	56	113.0	36.5	30.5	126.2	45.5	27.2	53.4
A4N	43	86.6	27.9	30.5	126.2	45.5	27.2	53.4
C1NC	52	104.9	33.8	33.5	165.7	46.6	27.7	59.1
C1S	43	56.6	27.9	33.5	165.7	46.6	27.7	59.1
A3SC	57	115.0	37.1	30.5	127.3	46.5	27.8	55.1
A3N	50	100.8	32.5	30.5	127.3	46.5	27.8	55.1
C2NC	40	80.6	26.0	33.5	166.4	47.1	27.9	60.0
C2S	49	98.8	31.9	33.5	166.4	47.1	27.9	60.0
C3NC	53	106.9	34.5	33.5	165.0	46.2	27.4	58.3
C3S	29	58.3	18.7	33.5	165.0	46.2	27.4	58.3
A2SC	57	115.0	37.1	30.5	126.9	46.0	27.5	54.1
A2N	29	58.3	18.7	30.5	126.9	46.0	27.5	54.1

Note: Subscript “max” indicates experimentally measured values, subscript “n” indicates design values

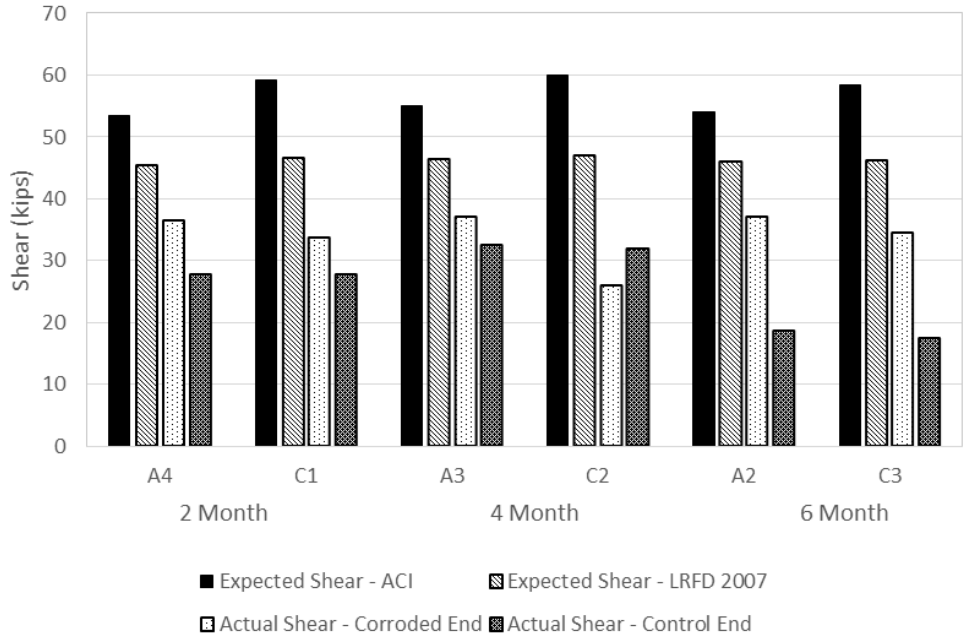

Figure 5. Estimated shear capacity compared to measured shear at failure for each specimen

Overall, the measured shear values were less than the design shear capacity calculated using the ACI and AASHTO LRFD 2007 methods for each girder. Most of the measured shear values were greater than the design shear capacity using the AASHTO LRFD 2012 method, which is known to be a conservative estimate due to simplifications in the equations relative to the iterative method used in AASHTO LRFD 2007. As noted earlier, the control ends of girder specimens A2 and C3, exposed for six months, had significantly smaller measured shear values than the other specimens, which were less than the design shear capacity using the AASHTO LRFD 2012 method. The corroded end of girder specimen C2, which was tested before the control end, unlike all the other specimens, also had a measured shear value less than the design shear capacity using the AASHTO LRFD 2012 method. The measured compressive strengths were used to calculate shear capacities, which should account for the variation in compressive strength related to estimated concrete shear strength. The *a/d* ratio used for all tests was 2.0, which puts the maximum shear stress at the edge of a discontinuity region, which is near the limiting value for the code methods. This may have reduced the applicability of the code equations. The strut and tie model was considered to account for the behavior of the discontinuity region. In each case the strength of the strut and tie model was governed by anchorage of the bottom tension tie. However, as is the case for strut and tie models, it provided a lower bound strength that was exceeded by the experimental values in all cases. Transfer and development lengths used during calculation of estimated capacity may have differed from the actual values due to variation in concrete compressive strength, which would affect the accuracy of the shear methods and the strut and tie model. Finally, the number of specimens examined is very small and variability between specimens could have a large influence on observed results.

CONCLUSIONS

The study described in this paper included laboratory investigation of the effect of corrosion on shear behavior of prestressed concrete members. Some corrosion is almost unavoidable near the ends of simply supported prestressed concrete bridge girders and corrosion becomes more of a problem when these ends are located beneath a leaking expansion joint. While many factors will influence the long-term performance of prestressed concrete girders, this corrosion may play a role in shear behavior of the members.

The following specific conclusions can be drawn from the results. Any differences in girder designs, concrete mix, bridge configurations, etc. could cause a variation from the results presented in this paper and therefore limit the applicability of the conclusions to similar situations.

1. The corroded ends of the members exhibited larger measured shear strengths for the conditions tested. The exact cause of these results is unclear, but can potentially be attributed to improved curing from the water used to induce corrosion or increased strand roughness without significant loss of section. Further research including deterioration to the point of strand section loss and concrete spalling, testing control ends before corroded ends, and examination of in-place concrete compressive strength is necessary to examine these hypotheses.
2. Strand slip was observed during all of the shear tests. The corroded girder ends exhibited strand slip prior to cracking and the control ends exhibited cracking prior to strand slip. This result indicates that corrosion may affect anchorage of the prestressing steel subjected to shear loading.
3. All specimens had experimental shear capacity less than the estimated values. The difference in measured and design shear strengths could be attributed to: the bond-shear failure mechanism, the variation in concrete compressive strength, an a/d ratio placing the load point at the edge of discontinuity region, and potential variations in transfer and development length related to compressive strength. A strut and tie model produced estimated strengths less than the experimental values, indicating that consideration of a model that better captures the bond behavior in the discontinuity region would produce a better estimate of capacity.

Further research is needed to address the questions raised by the results of this study, primarily related to the lower capacity of the non-corroded ends. The following items are recommended for future research:

1. The effect of testing order of the corroded and control ends on the shear capacity should be investigated further by examining similar specimens with the non-corroded ends tested first.
2. A larger number of specimens and more heavily corroded members with spalling concrete should be tested to better understand the effects of end region corrosion on shear capacity.
3. The effects of larger prestressing strands to be more susceptible to strand slip for the testing configuration used, causing the beam to potentially fail sooner should be

investigated further by constructing additional specimens using appropriately scaled prestressing strands.

REFERENCES

1. American Association of American Association of State Highway and Transportation Officials (AASHTO), AASHTO LFRD Bridge Design Specifications 6th Edition, American Association of State Highway and Transportation Officials (AASHTO), Washington, D.C., 2012,
2. Song, G. and Shayan, A. "Corrosion of steel in concrete: causes, detection and prediction: a state-of-the-art review," ARRB Transport Research Ltd. Review Report 4, 1998.
3. Coggins, F. B. and French, C. W. "Chloride Ion Distribution in Twenty-Year-Old Prestressed Bridge Girders," *ACI Materials Journal,* V. 87, No. 5, 1990, pp. 479-488.
4. Smith, J. L. and Virmani, Y. P. "Materials and Methods for Corrosion Control of Reinforced and Prestressed Concrete Structures in New Construction," FHWA-RD-00-081, U.S. Department of Transportation, Federal Highway Administration, McLean, VA, 2000.
5. Vu, K., Stewart, M. G., and Mullard, J. "Corrosion-Induced Cracking: Experimental Data and Predictive Models," *ACI Structural Journal,* V. 102, No. 5, 2005, pp. 719-726.
6. Abosrra, I., Ashour, A. F., and Youseffi, M. "Corrosion of Steel Reinforcement in Concrete of Different Compressive Strengths," *Construction and Building Materials,* V. 25, No. 10, 2011, pp. 3915-3925.
7. Bruce, S. M., McCarten, P. S., Freitag, S. A., and Hasson, L. M. "Deterioration of Prestressed Concrete Bridge Beams," Land Transport New Zealand Research Report 337, 2008.
8. Szilard, R. "Corrosion and Corrosion Protection of Tendons in Prestressed Concrete Bridges," *ACI Journal,* V. 66, No. 1, 1969, pp. 42-59.
9. Rogers, R. A., Wotherspoon, L., Scott, A., and Ingham, J. M. "Residual strength assessment and destructive testing of decommissioned concrete bridge beams with corroded pretensioned reinforcement," *PCI Journal,* V. 57, No. 3, 2012, pp. 100-118.
10. El-Batanouny, M. K., Mangual, J., Ziehl, P. H., and Matta, F. "Early Corrosion Detection in Prestressed Concrete Girders Using Acoustic Emission," *Journal of Materials in Civil Engineering,* V. 26, No. 3, 2014, pp. 504-511.
11. Pape, T. M. and Melchers, R. E. "Performance of 45-year-old corroded prestressed concrete beams," *Structures and Buildings,* V. 166, No. SB10, 2013, pp. 547-559.
12. Cranor, B. "Analysis and Experimental Testing for Shear Behavior of an AASHTO Type II Girder in Service for Several Decades," M.S. Thesis, The University of Oklahoma, Norman, OK, 2015.
13. ACI Committee 318, Building Code Requirements for Structural Concrete (ACI 318-14) and Commentary (ACI 318R-14), American Concrete Institute, Farmington Hills, MI, 2014.

14. Ray, I., Parish, G., Davalos, J., and Chen, A. "Effect of Concrete Substrate Repair Methods Aged by Accelerated Corrosion and Strengthened with CFRP," *Journal of Aerospace Engineering*, V. 24, No. 2, 2011, pp. 227-239.
15. Kaar, P., LaFraugh, R., and Mass, M. "Influence of Concrete Strength on Strand Transfer Length," *PCI Journal*, V. 8, No. 2, 1963, pp. 47-67.
16. Naji, B., Ross, B. E., Floyd, R. W. “Characterization of Bond-Loss Failures in Pretensioned Concrete Girders,” *Journal of Bridge Engineering*, V. 22, No. 4, 2017.
17. American Association of State Highway and Transportation Officials (AASHTO), LRFD Bridge Design Specifications Customary U.S. Units 4th Edition, American Association of State Highway and Transportation Officials (AASHTO), Washington, D.C., 2007.